Chemistry International 6(4) (2020) 267-276

International Scientific Organization
http://iscientific.org/
Chemistry International
www.bosaljournals.com/chemint/

Pipeline steel protection in oil well acidizing fluids using expired pharmaceutical agent

Nkem B. Iroha[1,*] and Ngozi J. Maduelosi[2]

[1]Electrochemistry and Material Science Unit, Department of Chemistry, Federal University Otuoke, Nigeria
[2]Department of Chemistry, Rivers State University, Port Harcourt, Nigeria
*Corresponding author's E. mail: irohanb@fuotuoke.edu.ng.com, nkemib@yahoo.com

ARTICLE INFO

Article type:
Research article
Article history:
Received January 2020
Accepted March 2020
October 2020 Issue
Keywords:
Expired Pregabalin
X60 pipeline steel
SEM analysis
Inhibition efficiency
Physisorption

ABSTRACT

The protection performance of expired Pregabalin for X60 pipeline steel corrosion in 15% HCl solution was investigated using weight loss technique, electrochemical measurements and scanning electron microscopy (SEM) analysis. The results show that Pregabalin inhibited the acid induced corrosion of X60 steel and its inhibition efficiency increases with inhibitor concentration. Polarization measurements indicate that the inhibitor act as mixed type inhibitor. Impedance measurements suggest that the corrosion reaction is controlled by charge transfer process. Weight loss measurements carried out at different temperature showed that adsorption of the expired drug involve physisorption mechanism. The adsorption followed the Langmuir isotherm with negative values of Gibbs free energy of adsorption, suggesting a stable and spontaneous inhibition process. SEM analysis confirmed the existence of a protective film of the inhibitor on X60 steel surface.

Capsule Summary: Corrosion inhibition effect of expired Pregabalin on X60 steel in 15% HCl solution has been investigated by weight loss and electrochemical techniques. It was found that the expired drug inhibited the acid induced corrosion of X60 steel and the inhibition efficiency increases with increase in concentration of the drug and decrease with rise in temperature.

Cite This Article As: N. B. Iroha and N. J. Maduelosi. Pipeline steel protection in oil well acidizing fluids using expired pharmaceutical agent. Chemistry International 6(4) (2020) 267-276. https://doi.org/10.5281/zenodo.3735669

INTRODUCTION

The protection of metals against corrosion has continued to dominate discussions, especially in the oil and gas industry where most lines are made of metals and the fact that common practices like acid pickling, acid descaling, acid cleaning, and oil well acidizing (usually done with mixtures containing 15% HCl solution) induce corrosion. Several methods have been devised for preventing or reducing corrosion, which include metal coating, inorganic coating, painting, as well as use of chemical inhibitors. Among all these methods, corrosion inhibitors are widely used and acts as one of the most economical and effective ways (Sherif et al., 2010; Obot and Obi-Egbedi, 2010; Raja and Sethuraman, 2008).Corrosion inhibition occurs via adsorption of their molecules on the corroding metal surface, and the efficiency of inhibition depends on the mechanical, structural and chemical characteristics of the adsorption layers formed under particular condition (Eddy et al., 2009). Most of the synthetic organic inhibitors are hazardous to health and cause adverse effect on environment (Iroha et al., 2015; Verma et al., 2015; Tang et al., 2010)

The development of efficient and effective corrosion inhibitors for industrial application still remains a subject of active research. The search for these inhibitors for metal

(a) (b)

Fig. 1: Structure of Pregabalin [3-isobutyl GABA, (S)-3-isobutyl-γ-aminobutyric acid], (a) Molecular structure (b) Optimized structure: N - blue; O-red; C-gray; H-white

corrosion in different aggressive media has taken a new dimension owing to the clarion call for green chemistry. Comparisons have been made over the years between the toxic inhibitors, like chromates and other organic inhibitors, with the natural inhibitors and it has been observed that the natural inhibitors could serve as an effective substitute for the currently preferred organic inhibitors; sometimes they show significantly better inhibitive properties than the currently employed organic corrosion inhibitors (Blajiev and Hubin, 2004; Valek and Martinez, 2007).

Recently pharmaceutical drugs were used as effective inhibitors of metal corrosion because of their non-toxic characteristics and negligible negative impacts on the aquatic environment (Gece, 2011; Iroha and James, 2019; Ahamad, 2010; Iroha and Nnanna, 2019).The protection ability of these drugs has been linked with their heterocyclic nature and the presence of oxygen, nitrogen and sulphur as active centers in their molecules (Eddy and Odoemelam, 2008; Iroha and Nnanna, 2019). However, most of the pharmaceutical drugs are more expensive than the organic inhibitors currently used in industries, which implies that using fresh drug as a corrosion inhibitor may not be economically viable (Vaszilcsin et al., 2012). Thus, it is worthwhile to investigate the corrosion inhibition properties of expired drugs which are of no use. It is reported that the active constituent of a drug degrades only infinitesimally and more than 90% of the drugs maintain stability long time after the expiration date (Gupta et al., 2017).

Pregabalin (PGB), marketed under the brand name Lyrica among others, is a medication used to treat epilepsy, neuropathic pain, fibromyalgia, restless leg syndrome, and generalized anxiety disorder (Frampton, 2014; Iftikhar et al., 2017). The molecular and optimized structures of Pregabalin are shown in Fig. 1. In this work the corrosion inhibiting effect of expired Pregabalin for X60 pipeline steel corrosion in 15% HCl solution was investigated using weight loss, potentiodynamic polarization (PDP) and electrochemical impedance spectroscopy (EIS) techniques. Scanning electron microscopy (SEM) was further employed to provide a pictorial representation in the surface to understand the nature of the surface film.

MATERIAL AND METHODS

Material preparation

The composition of X60 steel specimen used in this study was C 0.20wt%, Mn 1.16wt%, P 0.01wt%, Si 0.36wt%, Cr 0.082wt%, Mo 0.093wt%, Ni 0.098wt%, Al 0.018wt%, Co 0.013wt%, Cu 0.18wt%, Nb 0.018wt%, V 0.057wt%, and balance Fe. The X60 steel coupons used in weight loss and electrochemical experiments were mechanically cut into 3 x 2 x 0.15 and 2 x 2 x 0.15 cm dimensions respectively. These specimens were carefully prepared prior to each experiment. They were abraded with Si-C emery paper (600–1200 mesh size), washed with distilled water and then ethanol, degreased with acetone and finally stored in moisture free desiccators. The aggressive solution, 15% HCl was prepared by dilution of analytical grade 37% HCl solution with distilled water. The expired Pregabalin was gotten from Ebus Pharmacy and used as inhibitor without further purification. Several concentrations of the tested drug ranging from 1.0 to 2.5 g L^{-1} were used for gravimetric and electrochemical studies while the SEM study was carried out at 2.5 g L^{-1} concentration (optimum concentration).

Weight loss measurement

The weight loss measurement was achieved using the method described earlier (Iroha et al., 2012a). After weighing accurately, the specimens in triplicate were immersed in beakers containing 250 mL of 15% HCl solution with different concentrations of the tested expired drug for 4 h at 303, 313 and 323 K. At the end of exposure period, specimens were cleaned according to ASTM G-81 and their weight recorded. The corrosion rate (CR) values were determined according to Eq. 1.

$$CR = \frac{\Delta W \times 87600}{\rho A t} \qquad (1)$$

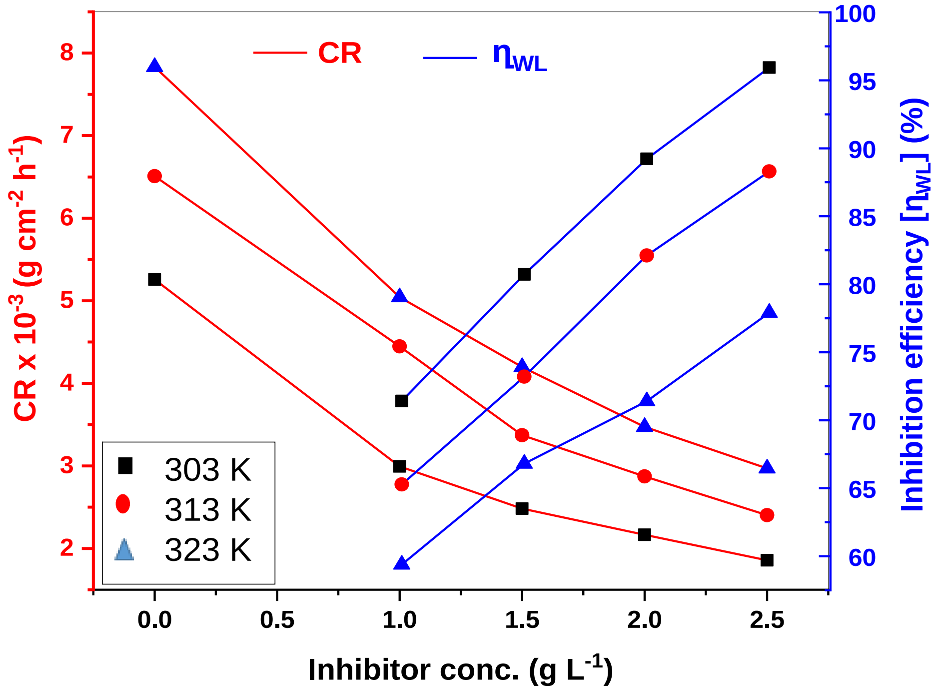

Fig. 2: Variation of X60 steel corrosion rate and inhibition efficiency with inhibitor concentration for PGB at different temperatures

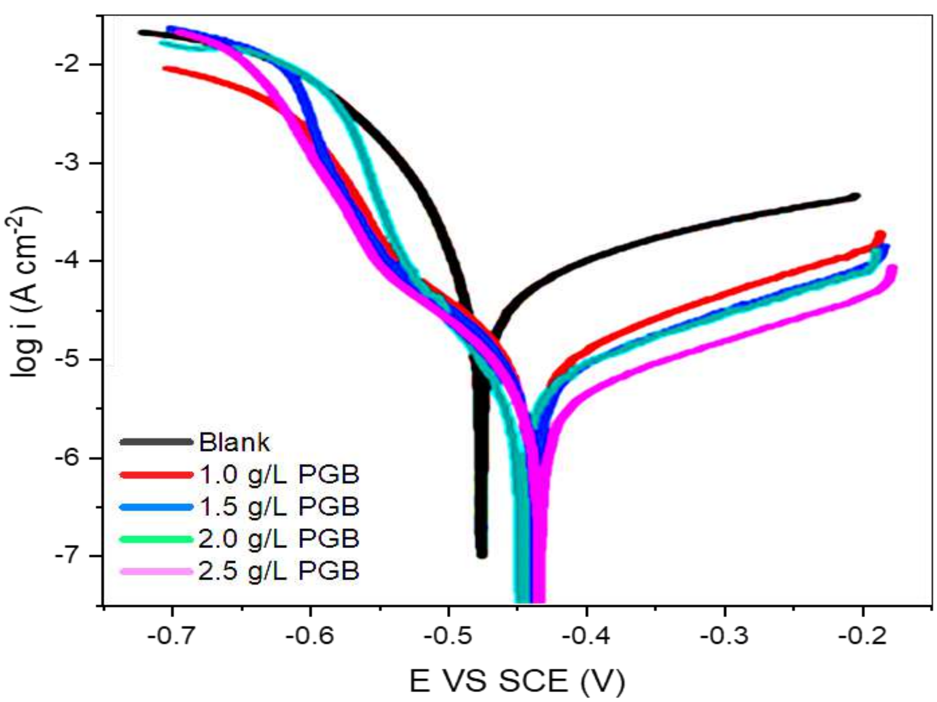

Fig. 3: Polarization curves for X60 steel corrosion in 15%HCl solution in the absence and presence of different concentrations of PGB

Where, ΔW is weight loss in gram (g), ρ is density of the metal coupons (g/cm^3), A is exposed surface area of the metal coupon (cm^2) and t is exposure time (h). The inhibition efficiency (η_{WL}%) of the expired PGB was evaluated using relation shown in Eq. 2.

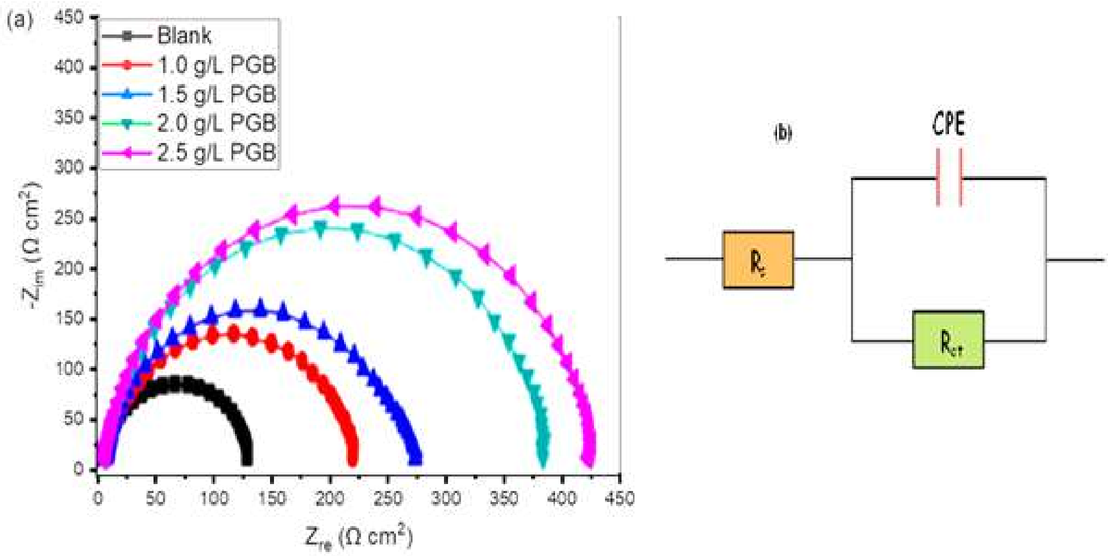

Fig. 4: (a) Nyquist plot of X60 steel in 15% HCl with different concentrations of PGB, (b) Equivalent circuit model used to fit Nyquist experimental data

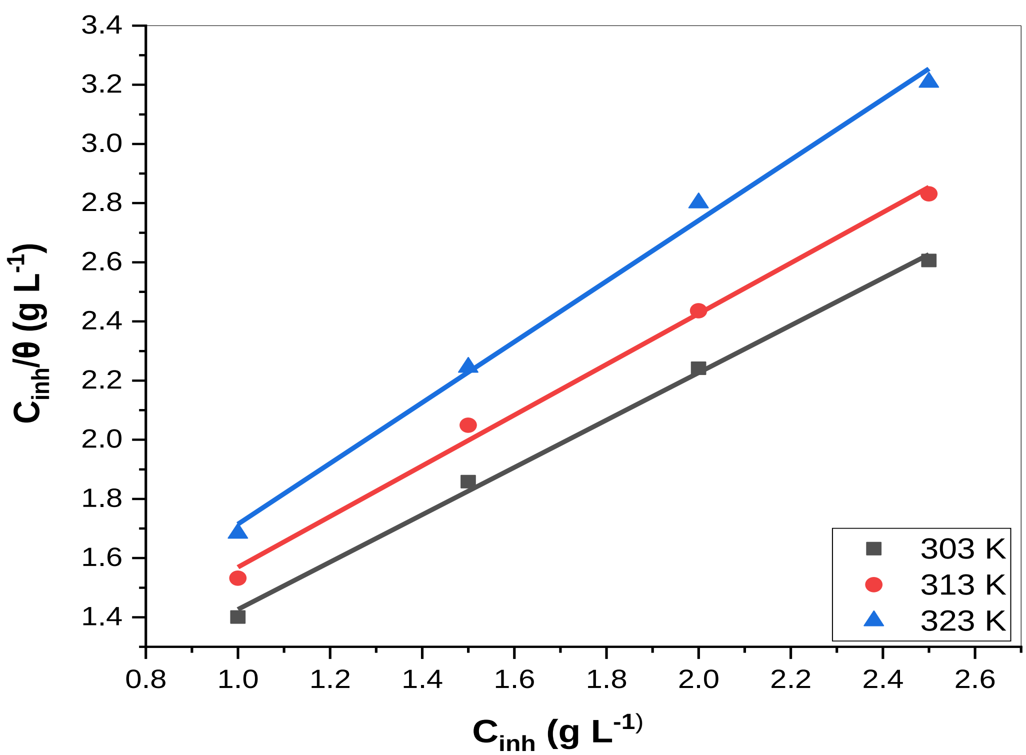

Fig. 5: Langmuir adsorption isotherm for PGB in 15% HCl at different temperatures

$$\eta_{WL}\% = \left(1 - \frac{CR_{(inh)}}{CR_{(blank)}}\right) \times 100 \quad (2)$$

Where, $CR_{(blank)}$ and $CR_{(inh)}$ are the corrosion rates of the X60 steel coupons in the absence and presence of inhibitor, respectively.

Electrochemical analysis

Electrochemical experiments are performed on Gamry Reference 3000 advanced electrochemical workstation in a conventional three electrode system including saturated calomel electrode as reference electrode, platinum electrode as counter electrode and X60 steel of a 1 cm^2 exposed area as working electrode. All experiments were performed at room temperature (30 ± 2°C) in 15% HCl electrolyte solution with and without PGB inhibitor. The working electrode was immersed in the test solution for 30 min to a establish steady state open circuit potential (E_{ocp}). All potentials were measured versus saturated calomel electrode. In order to get more accuracy and reproducibility of experimental data, the electrochemical studies were performed in triplicate at each tested concentration of the PGB and mean values are reported. For electrochemical impedance spectroscopic (EIS) studies, a sinusoidal voltage of amplitude 10 mV in a frequency range 10 kHz to 0.1 Hz was imposed. Inhibition efficiency (η_{EIS}%) from the EIS method was calculated using relation shown in Eq. 3.

$$\eta_{EIS}\% = \left(1 - \frac{R_{ct(B)}}{R_{ct(I)}}\right) \times 100 \quad (3)$$

Where, $R_{ct(B)}$ and $R_{ct(I)}$ were the charge transfer resistance with and without inhibitor, respectively. The potentiodynamic polarization (PDP) was measured at ±250 mV from E_{corr} with a scan rate of 1 mV/s (Gong et al., 2018; Iroha and James, 2019). The corrosion current density (i_{corr}) was calculated by extrapolating the linear segments of the cathodic and anodic Tafel slopes from which corrosion inhibition efficiency(η_{PDP}%) was calculated using Eq. 4.

$$\eta_{PDP}\% = \frac{i_{corr(B)} - i_{corr(I)}}{i_{corr(B)}} \times 100 \quad (4)$$

Where, $i_{corr(B)}$ and $i_{corr(I)}$ represent the corrosion current density values without and with different inhibitor concentration respectively.

SEM analysis

The surface morphology of the X60 steel specimens in the absence and the presence of optimum concentration of inhibitor were analyzed using Scanning Electron Microscopy (SEM; FEI Inspect S-50, Tokyo, Japan). The X60 steel coupons of size 3 x 2 x 0.15 cm were immersed in 15% HCl in absence and presence of optimum concentration (2.5 g L^{-1}) of PGB for 4 h. Thereafter, the X60steel specimens were taken out, washed with double distilled water, dried and finally analyzed by SEM.

RESULTS AND DISCUSSION

Weight loss tests

Fig. 2 illustrates the variation of corrosion rate and inhibition efficiency with inhibitor concentration at different temperatures. The curves shows increase in inhibition efficiency with increase in PGB concentration accompanied by a significant decrease in corrosion rate. This trend may result from the fact that the adsorption of PGB on the X60 steel increases with the increase in inhibitor concentration thus the X60 steel surface is efficiently separated from the medium by the formation of a film on its surface (Iroha et al., 2005; Aljourani, 2009).An increase in corrosion rate with rise in temperature is observed while inhibition efficiency is found to decrease with rise in temperature, suggesting that PGB was physically adsorbed on the metal surface (Iroha et al., 2012b).

Polarization curves

Fig. 3 presents the potentiodynamic polarization curves of X60 steel in 15%HCl without and with the studied inhibitor at 303 K. Their extracted electrochemical parameters are given in Table 1.The percentage inhibition efficiency (η_{PDP}%) of the expired PGB calculated using equation 4 is also shown in the table.It is observed that the addition of the expired PGB suppresses both anodic metal dissolution and the cathodic hydrogen evolution reactions; it causes E_{corr} to shift slightly towards more positive values as well as decrease the magnitudes of the anodic and cathodic current densities. Furthermore, the variation in E_{corr} is slight, with a maximum shift of about 29 mV (vs. SCE). This observation indicates that the inhibitor could be classified as mixed type inhibitor. Inspection of Table 1 reveals that the values of cathodic Tafel slope, β_c, and anodic Tafel slope, β_a, are slightly changed with increasing inhibitor concentration, indicating the influence of the PGB on the kinetics of hydrogen evolution and the steel dissolution mechanism. The data in Table 1 also shows that the corrosion current density (i_{corr}) decreases, and the inhibition efficiency (η_{PDP}%) increases as the concentration of PGB is increased. This indicates that the addition of PGB inhibits the corrosion process by decreasing the surface area for corrosion.

Electrochemical impedance spectroscopy

Electrochemical impedance spectroscopy has been used to confirm the formation of protective film on the X60 steel surface. The Nyquist plots for X60 steel corrosion in 15% HCl are presented in Fig. 4a. From Fig. 4a, it can be observed that the Nyquist plots in the presence of PGB are similar to the blank one, indicating that the inhibitors took control of the activation of the electrochemical reaction without changing the reaction mechanism to prevent the corrosion behavior of steel (Xu et al., 2016; Ji et al., 2016).

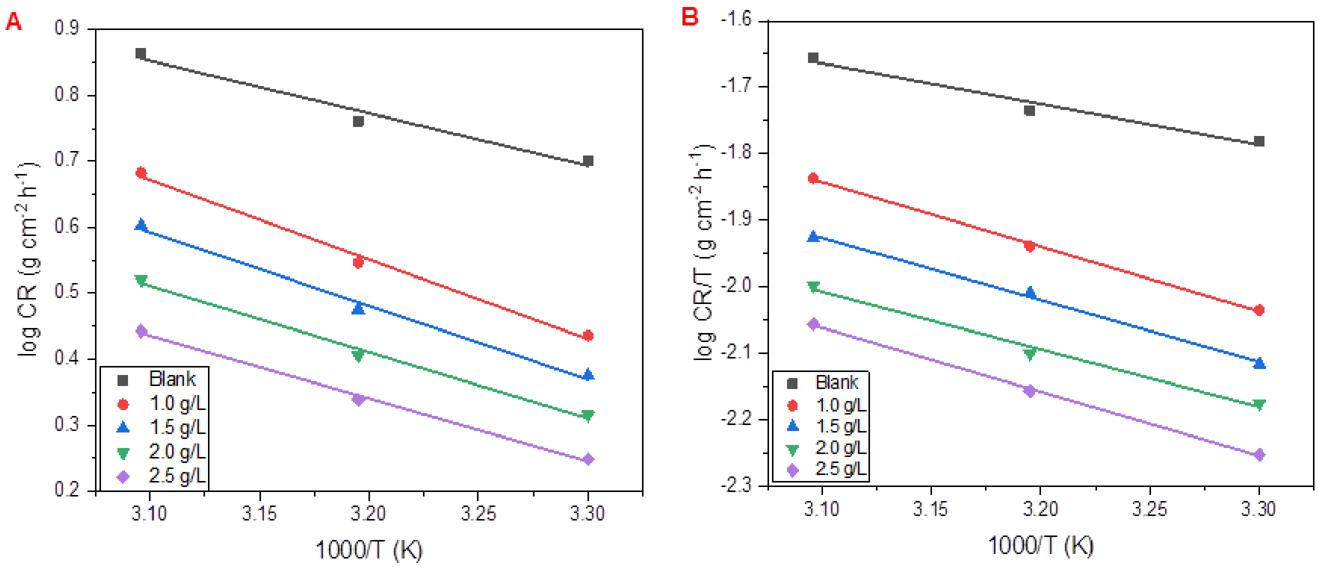

Fig. 6: (a) Arrhenius plots for X60 steel in 15% HCl without and with various concentrations of PGB and (b) Transition state plots for X60 steel in 15% HCl without and with various concentrations of PGB

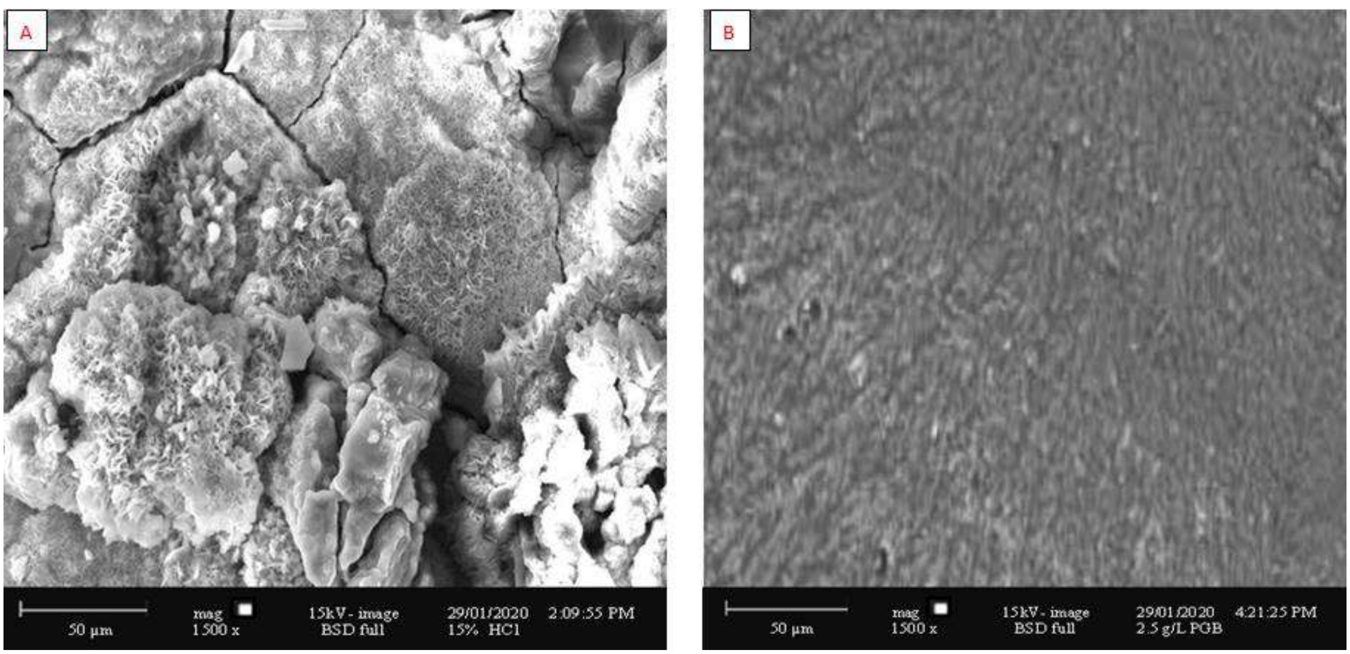

Fig. 7: SEM pictures of X60 steel in (a) free 15% HCl solution and (b) presence of 2.5 g/L PGB after 4 h immersion time at 303 K.

A depressed semi-circle capacitive loop, as often obtained in acidic media (Hamilton-Amachree and Iroha, 2020) can be seen. From the shape of the loop it can be inferred that corrosion of X60 steel is controlled by charge transfer process. The diameter of the capacitive loop increases with increasing concentration of PGB inhibitor. These results suggest that a protective film is formed on the metal surface and is enhanced with the concentration of PGB.

The obtained Nyquist impedance plots were analysed by fitting the experimental data to a simple equivalent circuit model (Fig. 4b), which includes the solution resistance R_s and the constant phase element

(CPE) together with the charge transfer resistance element R_{ct} (Ehteram and Al-Moubaraki, 2008; Iroha and Chidiebere, 2017). The use of a CPE in place of double layer capacitance (C_{dl}), accounts for the deviations from ideal dielectric behaviour and is related to surface inhomogeneities. The impedance (Z_{CPE}) of the CPE can be represented as shown in Eq. 5.

$$Z_{CPE} = Y_0^{-1}(j\omega)^{-n} \quad (5)$$

Where, Y_0 is the CPE constant, ω is the angular frequency; j is the imaginary number (i.e. $j^2=-1$) and n is the phase shift (exponent) which is related to the degree of surface inhomogeneity.The values of the double layer capacitance (C_{dl}) were calculated from the values of CPE constant (Y_0), angular frequency (ω) and phase shift (n) using Eq. 6.

$$C_{dl} = Y_0(\omega_{\max})^{n-1} \quad (6)$$

Where, ω_{max} is the frequency at which the imaginary part of impedance has attained the highest value (rad s^{-1}). The calculated EIS parameters from the Nyquist plots are given in Table 2.A careful inspection of the data in Table 2 reveals that the presence of different concentrations of expired PGB increases the values of R_{ct} which could be as a result of increased surface coverage on X60 steel by the inhibitor molecules (James and Iroha, 2019; Roy et al., 2014). The C_{dl} values in the presence of the inhibitor are generally lower than that of the blank acid system. The decrease in C_{dl} is due to an increase in the electrochemical double layer thickness or a reduction of the local dielectric constant, which is attributed to the adsorption of inhibitor molecules on the X60 steel surface (Zarrouk et al., 2015). The values of inhibition efficiency increased with increasing concentration of PGB to reach the optimum values of 92.4% at 2.5 g L^{-1}.

Adsorption isotherm

Based on the assumption, that the mechanism by which organic compounds inhibit metal corrosion is the adsorption of organic molecules on the metallic surface, then the surface coverage (θ) can be estimated from the inhibitor efficiency as; θ = η(%)/100. The adsorption characteristics of expired PGB was investigated by fitting data obtained for the degree of surface coverage of the inhibitor into various adsorption isotherms namely Freundlich, Langmuir, El- Awardy, Temkin, Flory Huggins and Frumkin adsorption isotherms. The Langmuir adsorption isotherm (Eq. 7) provided acceptable linear fits based on the near unity values of the correlation coefficient (R^2) values.

$$\frac{C_{inh}}{\theta} = \frac{1}{K_{ads}} + C_{inh} \quad (7)$$

Where, C is the concentration of PGB; θ is the surface coverage, which has been calculated from weight loss results; K_{ads} is the adsorptive equilibrium constant (Li et al., 2015; Zheng et al., 2014). Fig. 5, show straight lines of C_{inh}/θ against C_{inh} at all studied temperatures. Values of adsorption parameters deduced from Langmuir adsorption isotherm are recorded in Table 3.Higher values of K_{ads} (Table 3) suggest stronger adsorption of the inhibitor molecules on the metal surface and hence better inhibition efficiency (Saleh and Atia, 2006). The K_{ads} values decrease with increase in temperature indicating decrease in adsorption strength, probably due to desorption of the inhibitor molecules.The values of K_{ads} were used to calculate the value of the standard free energy of adsorption (ΔG^0_{ads}) using the expression shown in Eq. 8 (James and Iroha, 2019).

$$\Delta G^0_{ads} = -RT \ln(K_{ads} \times 55.5) \quad (8)$$

Where, R is the universal gas constant and the value 55.5 is the molar concentration of water in the solution. The negative sign of ΔG^0_{ads} in Table 3 indicate that adsorption of the studied compound on the X60 steel surface was spontaneous. Literature shows that, the standard Gibbs free energy of adsorption in aqueous solution with a value up to -20kJ/mol or less negative indicates physisorption while if the value is close to -40kJ/mol or more negative indicates chemisorption. The ΔG^0_{ads} values obtained in the present study range from −9.53 to −10.18 kJ mol^{-1}, which suggests that the adsorption of PGB on X60 steel surface is physisorption.

Corrosion kinetics analysis

The effect of temperature on the corrosion rate of X60 steel in 15% HCl containing different concentrations from expired PGB was tested by weight loss measurements over a temperature range from 303 to 323 K. Activation parameters were employed to give some insight about the inhibition and adsorption mechanism. Consequently, the corrosion kinetics parameters, namely, activation energy (E_a), activation enthalpy (ΔH^*), and activation entropy (ΔS^*) were calculated from the Arrhenius and transition state equations represented in relations 9 and 10, respectively.

$$\log CR = \frac{-E_a}{2.303RT} + \log A \quad (9)$$

$$\log \frac{CR}{T} = -\frac{\Delta H^*}{2.303RT} + \left\langle \log \frac{R}{Nh} + \frac{\Delta S^*}{2.303R} \right\rangle \quad (10)$$

Where, A is the pre-exponential factor, h is Plank's constant, N is Avogadro's number and other terms retain their previous meaning. The Arrhenius plots of log CR versus 1/T for the blank and different concentrations of PGB gave a straight line and a slope equal to $-E_a/2.303R$ shown in Fig. 6a, from which the values of E_a for the inhibited corrosion reaction of X60 steel have been calculated and recorded in Table 4.A plot of log CR/T against 1/T gives straight lines with slope values of ($\Delta H^*/2.303R$)) and an intercept of [log (R/Nh)) + ($\Delta S^*/2.303R$)] as in Fig. 6b, from which the values of ΔH^* and ΔS^* were calculated and given in Table 4.The data in Table 4 show that the values of E_a in the solution containing different concentrations of PGB are lower than that of the uninhibited solution, indicating strong adsorption of the inhibitor molecules on the metal surface and the presence of this additive induces the adsorption of its molecules on the surface of X60 steel. The endothermic nature of steel dissolution is indicated by the positive values of ΔH^* for the corrosion processes with and without the inhibitor. Values of the entropy of activation ΔS^* in the absence and in presence of the studied compound are negative. Large and negative values of entropies (ΔS^*) on increasing the inhibitor concentration imply that the activated complex in the rate determining step indicate an association rather than a dissociation step, meaning that a decrease in disordering takes place on going from reactants to the activated complex.

Surface morphology analysis

The scanning electron microscope images were recorded to establish the interaction of inhibitor with the metal surface, and they are shown in Fig. 7 (a, b). Fig. 7a depicts the SEM image of X60 steel surface in free acid solution which revealed a very rough surface with characteristic pits and cracks along with strongly damaged surface, due to the strong attack of 15% HCl solution. In the presence of PGB (Fig. 7b), the X60 steel surface was much less damaged with

Table 1: Potentiodynamic polarization parameters of X60 steel in 15% HCl with and without various concentrations of PGB at 303 K

Conc. of PGB (g L^{-1})	$-E_{corr}$ (mV vs SCE)	I_{corr} (μA cm^{-2})	b_a (mV dec^{-1})	b_c (mV dec^{-1})	η_{PDP} (%)
Blank	461.8	1872	171	163	-
1.0	470.8	624	165	159	66.7
1.5	477.2	492	168	153	73.7
2.0	483.9	297	151	149	84.1
2.5	491.0	159	168	155	91.5

Table 2: Impedance data of X60 steel in absence and presence of different concentrations of PGB at 303 K

Conc. of PGB (g L^{-1})	R_s (Ω cm^2)	R_{ct} (Ω cm^2)	n	Y_o (μ $\Omega^{-1}s^2cm^{-2}$)	C_{dl} (μFcm^{-2})	%η_{EIS} (%)
Blank	2.71	29.8	0.913	452.5	90.41	-
1.0	3.90	91.4	0.892	354.0	39.34	67.4
1.5	4.52	129.3	0.906	336.1	17.53	77.0
2.0	4.33	285.2	0.881	308.5	9.41	89.6
2.5	5.04	391.7	0.878	287.6	3.75	92.4

Table 3: Adsorption parameters of expired PGB at different temperatures

Temperature (K)	R^2	K_{ads} (g^{-1} L)	ΔG^o_{ads} (kJmol^{-1})
303	0.9971	1.0251	-10.18
313	0.9949	0.8741	-10.10
323	0.9948	0.6254	-9.53

Table 4: Activation Parameters of X60 Steel in 15% HCl solution in the absence and presence of different concentrations of PGB

Conc. of PGB (g/L)	E_a (kJ/mol)	ΔH^*(kJ/mol)	ΔS^* (J/mol/K)
Blank	97.39	78.31	-219.36
1.0	89.01	70.22	-229.18
1.5	85.58	66.83	-240.02
2.0	83.36	63.40	-254.69
2.5	81.52	60.93	-263.83

relatively smooth morphology, which shows the slowing down of the corrosion attack and the formation of a protective inhibitor film on the steel surface. Results revealed that the expired Pregabalin is highly efficient to inhibit the corrosion, which is a major issue worldwide (Askari et al., 2019; El Amine Ben Seghier et al., 2019; Ngobiri and Li, 2017; Ngobiri and Okorosaye-Orubite, 2017; Obot et al., 2019a; Obot et al., 2019b; Ohaeri et al., 2019; Onyeachu et al., 2019; Ukpaka and Uku, 2018) and Pregabalin could possibly be used for oilfield application to inhibit the pipeline steel corrosion.

CONCLUSIONS

In summary, this work has investigated the inhibition effect of expired Pregabalin (PGB) on X60 pipeline steel corrosion in 15%HCl solution. The expired PGB was found to be a good eco-friendly corrosion inhibitor for X60 steel in the aid solution and its inhibition efficiency increases with increasing concentration and decreases with increase in temperature. The adsorption of PGB on X60 steel obeyed the Langmuir adsorption isotherm and occurred via physisorption mechanisms. Potentiodynamic polarization study confirms the results obtained from weight loss method and revealed that PGB functions as a mixed–type corrosion inhibitor. EIS data revealed a decrease in C_{dl} values due to a decrease in the local dielectric constant or an increase in thickness of the electrical double layer, indicating the formation of adsorbed film of the inhibitor molecules on the steel surface. SEM analysis showed the reduction in damage of the X60 steel in the presence of the inhibitor.

REFERENCES

Ahamad, I., Prasad, R., Quraishi, M.A., 2010. Inhibition of mild steel corrosion in acid solution by Pheniramine drug: Experimental and theoretical study. Corrosion Science 52, 3033–3041.

Aljourani, J., Raeissi, K., Golozar, M.A., 2009. Benzimidazole and its derivatives as corrosion inhibitors for mild steel in 1M HCl solution, Corrosion Science 51, 1836-1843.

Askari, M., Aliofkhazraei, M., Afroukhteh, S., 2019. A comprehensive review on internal corrosion and cracking of oil and gas pipelines. Journal of Natural Gas Science and Engineering 71, 102971.

Blajiev, O., Hubin, A., 2004. Inhibition of copper corrosion in chloride solutions by amino-mercapto-thiadiazol and methyl-mercapto-thiadiazol: an impedance spectroscopy and a quantum-chemical investigation. Electrochimia Acta 49, 2761–2770.

Eddy, N.O., Ibok, U.J., Ebenso, E.E., 2009. Adsorption, synergistic inhibitive effect and quantum chemical studies on ampicillin and halides for the corrosion of mild Steel in H_2SO_4. Journal of Applied Electrochemistry 40, 445–456.

Eddy, N.O., Odoemelam, S.A., 2008. Norfloxacin and sparfloxacin as corrosion inhibitors for zinc: Effect of concentrations and temperature. Journal of Material Science 4, 87-96.

Ehteram, A.N., Al-Moubaraki, A.H., 2008. Corrosion behavior of mild steel in hydrochloric acid solutions. International Journal of Electrochemcal Science 3, 806-818.

El Amine Ben Seghier, M., Keshtegar, B., Correia, J.A.F.O., Lesiuk, G., De Jesus, A.M.P., 2019. Reliability analysis based on hybrid algorithm of M5 model tree and Monte Carlo simulation for corroded pipelines: Case of study X60 Steel grade pipes. Engineering Failure Analysis 97, 793-803.

Frampton, J.E., 2014. Pregabalin: A review of its use in adults with generalized anxiety disorder. CNS Drugs 28(9), 835–854.

Gece, G., 2011. Drugs: a review of promising novel corrosion inhibitors. Corrosion Science 53, 3873–3898.

Gong, Z., Peng, S., Huang, X., Gao, L., 2018. Investigation of the corrosion inhibition effect of Itraconazole on copper in H_2SO_4 at different temperatures: Combining experimental and theoretical studies. Materials 11, 2107-2128.

Gupta, N.K., Gopal, C.S.A., Srivastava, V., Quraishi, M.A., 2017. Application of expired drugs in corrosion inhibition of mild steel. International Journal of Pharmaceutical Chemistry and Analysis 4(1), 8-12.

Hamilton-Amachree, A., Iroha, N.B., 2020. Corrosion inhibition of API 5L X80 pipeline steel in acidic environment using aqueous extract of *Thevetia peruviana*. Chemistry International 6(3), 117-128.

Iftikhar, I.H, Alghothani, L., Trotti, L.M., 2017. Gabapentin enacarbil, pregabalin and rotigotine are equally effective in restless legs syndrome: a comparative meta-analysis. European Journal of Neurology 24(12), 1446–1456

Iroha N.B., Akaranta O., James A.O., 2012b. Red onion skin extract-furfural resin as corrosion inhibitor for aluminium in acid medium. Der Chemica Sinica 3(4), 995-1001.

Iroha N.B., James A.O., 2019. Adsorption behavior of pharmaceutically active dexketoprofen as sustainable corrosion Inhibitor for API X80 carbon steel in acidic medium. World News of Natural Sciences 27, 22-37.

Iroha, N.B., Akaranta, O., James, A.O., 2012a. Corrosion inhibition of mild steel in acid media by red peanut skin extract-furfural resin. Advances in Applied Science Research 3(6), 3593-3598.

Iroha, N.B., Akaranta, O., James, A.O., 2015. Red onion skin extract-formaldehyde resin as corrosion inhibitor for mild steel in hydrochloric acid solution. International Research Journal of Pure and Applied Chemistry 6(4), 174-181.

Iroha, N.B., Chidiebere, M.A., 2017. Evaluation of the inhibitive effect of *Annona muricata* l leaves extract on low-carbon steel corrosion in acidic media. International Journal of Materials and Chemistry 7(3), 47-54.

Iroha, N.B., Nnanna, L.A., 2019. Electrochemical and Adsorption Study of the anticorrosion behavior of

Cefepime on Pipeline steel surface in acidic Solution, Journal of Materials and Environmental Sciences 10(10), 898-908.

Iroha, N.B., Oguzie, E.E., Onuoha, G.N, Onuchukwu, A.I., 2005. Inhibition of mild steel corrosion in acidic solution by derivatives of diphenyl glyoxal. 16th International Corrosion Congress, Beijing, China, 126-131.

James, A.O., Iroha, N.B., 2019. An investigation on the inhibitory action of modified almond extract on the corrosion of Q235 mild steel in acid environment. IOSR Journal of Applied Chemistry, 12(2), 01-10.

Ji, Y., Xu, B., Gong, W., Zhang, X., Jin, X., Ning, W., Meng, Y. Yang, W. and Chen, Y., 2016. Corrosion inhibition of a new Schiff base derivative with two pyridine rings on Q235 mild steel in 1.0 M HCl. Journal of the Taiwan Institute of Chemical Engineers 66, 301–312.

Li, X., Xie, X., Deng, S., Du, G., 2015.Inhibition effect of two mercaptopyrimidine derivatives on cold rolled steel in HCl solution. Corrosion Science 92, 136-147.

Ngobiri, N., Li, Y., 2017. Inhibition of pipeline steel corrosion in acidic environment using sulphadoxine and pyrimethamine. Chemistry International 3, 114-122.

Ngobiri, N., Okorosaye-Orubite, K., 2017. Adsorption and corrosion inhibition characteristics of two medicinal molecules. Chemistry International 3, 185.

Obot, I.B., Obi-Egbedi, N.O., 2010. Adsorption properties and inhibition of mild steel corrosion in sulphuric acid solution by ketoconazole: Experimental and theoretical investigation. Corrosion Science 52(1), 198-204.

Obot, I.B., Onyeachu, I.B., Umoren, S.A., 2019a. Alternative corrosion inhibitor formulation for carbon steel in CO2-saturated brine solution under high turbulent flow condition for use in oil and gas transportation pipelines. Corrosion Science 159, 108140.

Obot, I.B., Umoren, S.A., Ankah, N.K., 2019b. Pyrazine derivatives as green oil field corrosion inhibitors for steel. Journal of Molecular Liquids 277, 749-761.

Ohaeri, E., Eduok, U., Szpunar, J., 2019. Relationship between microstructural features in pipeline steel and hydrogen assisted degradation. Engineering Failure Analysis 96, 496-507.

Onyeachu, I.B., Obot, I.B., Sorour, A.A., Abdul-Rashid, M.I., 2019. Green corrosion inhibitor for oilfield application I: Electrochemical assessment of 2-(2-pyridyl) benzimidazole for API X60 steel under sweet environment in NACE brine ID196. Corrosion Science 150, 183-193.

Raja, P.B., Sethuraman, M.G., 2008. Natural products as corrosion inhibitor for metals, in corrosive media: A review. Materials Letters 62, 113–116.

Roy, P., Karfa, P., Adhikari, U., Sukul, D., 2014. Corrosion inhibition of mild steel in acidic medium by polyacrylamide grafted Guar gum with various grafting percentage: Effect of intramolecular synergism. Corrosion Science 88, 246–253.

Saleh, M.M., Atia, A.A., 2006. Effects of structure of the ionic head of cationic surfactant on its inhibition of acid corrosion of mild steel. Journal of Applied Electrochemistry 36, 899–905.

Sherif, S.M., Erasmus, R.M., Comines, J.D., 2010. Effects of 5-(3-aminophenyl)-tetrazole as a corrosion inhibitor on the corrosion of Mg/Mn alloy in Arabian Gulf water. Electrochimica Acta 55(11), 3657-3663.

Tang, Y., Yang, X., Yang, W., Chen, Y., Wan, R., 2010. Experimental and molecular dynamics studies on corrosion inhibition of mild steel by 2-amino-5-phenyl-1,3,4-thiadiazole. Corrosion Science 52, 242–249.

Ukpaka, C.P., Uku, P.E., 2018. Application of mathematical tools and techniques in monitoring and predicting stainless steel corrosion in river water media environment. Chemistry International 4, 77-84.

Valek, L., Martinez, S., 2007. Copper corrosion inhibition by Azadirachtaindica leaves extract in 0.5 M sulphuric acid. Material Letters 61, 148–151.

Vaszilcsin, N., Ordodi, V., Borza, A., 2012.Corrosion inhibitors from expired drugs. International Journal of Pharmaceutics 431, 241-244.

Verma, C., Singh, A., Pallikonda, G., Chakravarty, M., Quraishi, M.A., Bahadur, I., Ebenso, E.E., 2015. Aryl sulfonamidomethylphosphonates as new class of green corrosion inhibitors for mild steel in 1 M HCl: electrochemical, surface and quantum chemical investigation, Journal of Molecular Liquids 209, 306–319.

Xu, B., Ji, Y., Zhang, X., Jin, X. Yang, W., Chen, Y., 2016. Experimental and theoretical evaluation of N, N-Bis(2-pyridylmethyl)aniline as a novel corrosion inhibitor for mild steel in hydrochloric acid. Journal of the Taiwan Institute of Chemical Engineers 59, 526–535.

Zarrouk, A., Hammouti, B., Lakhlifi, T., Traisnel, M.,Vezin, H., Bentiss, F., 2015. New 1H-pyrrole-2,5-dione derivatives as efficient organic inhibitors of carbon steel corrosion in hydrochloric acid medium: Electrochemical, XPS and DFT studies. Corrosion Science 90, 572–584.

Zheng, X., Zhang, S., Li, W., Yin, L., He, J., Wu, J., 2014. Investigation of 1-butyl-3-methyl-1H-benzimidazolium iodide as inhibitor for mild steel in sulfuric acid solution. Corrosion Science 80, 383-392.

Visit us at: http://bosaljournals.com/chemint/
Submissions are accepted at: editorci@bosaljournals.com